J Mater Sci: Mater Med (2009) 20:1619–1627
DOI 10.1007/s10856-009-3736-y

Application of impedance spectroscopy to evaluate the effect of different setting accelerators on the developed microstructures of calcium phosphate cements

H. E. Romeo · P. R. Bueno · M. A. Fanovich

Received: 22 August 2008 / Accepted: 17 March 2009 / Published online: 4 April 2009

Abstract The main goal of the present study was to evaluate the effect of different setting accelerator agents on the developed microstructures of calcium phosphate cements (CPCs) by employing the impedance spectroscopy (IS) technique. Six compositions of CPCs were prepared from mixtures of commercial dicalcium phosphate anhydrous (DCPA) and synthesized tetracalcium phosphate (TTCP) as the solid phases. Two TTCP/DCPA molar ratios (1/1 and 1/2) and three liquid phases (aqueous solutions of Na_2HPO_4, tartaric acid (TA) and oxalic acid (OA), 5% volume fraction) were employed. Initial (I) and final (F) setting times of the cement pastes were determined with Gillmore needles (ASTM standard C266-99). The hardened samples were characterized by X-ray powder diffraction (XRD), Fourier transformed infrared (FTIR) spectroscopy, scanning electron microscopy (SEM), and apparent density measurements. The IS technique was employed as a non-destructive tool to obtain information related to porosity, tortuosity and homogeneity of the cement microstructures. The formulation prepared from a TTCP/DCPA equimolar mixture and OA as the liquid phase presented the shortest I and F (12 and 20 min, respectively) in comparison to the other studied systems. XRD analyses revealed the formation of low-crystallinity hydroxyapatite (HA) (as the main phase) as well as the presence of little amounts of unreacted DCPA and TTCP after 24 h hardening in 100% relative humidity. This was related to the proposed mechanisms of dissolution of the reactants. The bands observed by FTIR allowed identifying the presence of calcium tartrate and calcium oxalate in the samples prepared from TA and OA, in addition to the characteristic bands of HA. High degree of entanglement of the formed crystals was observed by SEM in samples containing OA. SEM images were also correlated to the apparent densities of the hardened cements. Changes in porosity, tortuosity and microstructural homogeneity were determined in all samples, from IS results, when the TTCP/DCPA ratio was changed from 1/1 to 1/2. The cement formulated from an equimolar mixture of TTCP/DCPA and OA as the liquid phase presented setting times, degree of conversion to low-crystallinity HA and microstructural features suitable to be used as potential bone cement in clinical applications. The IS technique was shown to be a very sensitive and non-destructive tool to relate the paste composition to the developed microstructures. This approach could be very useful to develop calcium phosphate bone cements for specific clinical demands.

H. E. Romeo (✉) · M. A. Fanovich
Institute of Materials Science and Technology (INTEMA), University of Mar del Plata and National Research Council (CONICET), J. B. Justo 4302, 7600 Mar del Plata, Argentina
e-mail: hromeo@fi.mdp.edu.ar

P. R. Bueno
Instituto de Química, Universidade Estadual Paulista, P.O. Box 355, 14801-907 Araraquara, SP, Brazil

1 Introduction

A self-setting cement consisting of only calcium phosphate compounds has been developed by Brown and Chow [1]. The major components of this calcium phosphate cement (CPC) are tetracalcium phosphate ($Ca_4(PO_4)_2O$, TTCP) and dicalcium phosphate anhydrous ($CaHPO_4$, DCPA). These components can be mixed with water to form a paste that can be employed to fill any osseous defect whatever its shape. The paste sets in vivo to produce hydroxyapatite ($Ca_{10}(PO_4)_6(OH)_2$, HA), the main mineral component in teeth and bones. These CPCs have been shown to be

biocompatible and bioconductive with soft and hard tissues because of the apatitic nature of the setting reaction products. The CPCs are widely used for bone regeneration in different fields as an alternative to sintered bioceramics, leading to a final product more reactive than the sintered one and more similar to the biological apatites [2–6].

These cements consist of a mixture of a powder (mixture of calcium phosphates) and a liquid phase containing an accelerator agent. Different setting accelerators have been employed in TTCP–DCPA based cements, among which, aqueous solutions of acids [7] and salts [5, 8] were the most commonly used. Once the cement paste is formed, it sets in situ as a result of dissolution and precipitation processes which take place during the first stages of the hydration of the CPC. Finally, the entanglement of the formed crystals leads to the hardening of the cement. The chemical reactions that take place during the setting of a CPC depend on its chemical composition as well as on the pH of the system. However, despite the numerous publications, some basic aspects of these bone cements, such as the influence of different kinds of accelerator agents and TTCP/DCPA molar ratios on the setting times and microstructural features, are not well understood yet [9]. In this way, different accelerator solutions have been employed in order to decrease both initial and final setting times without deteriorating the mechanical properties of the cements [10–12].

It is well known that, as a result of setting and hardening mechanisms in these cements, an intrinsic microporosity is originated. Concerning this issue, the porosity and other microstructural parameters (e.g. tortuosity) of the cements play a very important role, for instance, on the kinetics of drug release [13] as well as on cell infiltration for bone ingrowth. Nevertheless, there are no studies that analyse deeply the influence of the nature of the accelerator used in these CPCs on the microporosity and tortuosity of the hardened material. In this context, we propose the characterization of these structural features by using the impedance spectroscopy (IS) technique. In recent years, this technique has been successfully used to evaluate the hydration process of Portland cement [14–16], and it has been shown that this technique is a very sensitive tool to reveal changes in the microstructure, mainly concerning porosity and connectivity of the cement matrix, among others [17].

The aim of the present work was to evaluate the influence of the nature of three different setting accelerators (aqueous solutions of disodium hydrogen phosphate, tartaric acid and oxalic acid) on the developed microstructural features of CPCs by employing impedance spectroscopy. Solutions of disodium hydrogen phosphate have been widely used as accelerants of cement systems of the type TTCP–DCPA [8]. For that reason, it was choosen as a reference solution. On the other hand, tartaric acid has been shown to easily form calcium tartrate when it reacts with calcium ions. As a consequence, we decided to employ it as a potential hardening accelerator as a result of the precipitation of the tartrate salt. In particular, oxalic acid solutions have been employed as setting accelerants of glass-ionomer cements [18], however, this organic acid has not been employed yet as a setting accelerator of a CPC. For this reason, we proposed the incorporation of this organic acid as a potential setting accelerant of a CPC, on the base of its pH lowering effect (this would lead to the release of ions from the calcium phosphate reactants) and its possibility of forming insoluble salts with calcium ions. The prepared cements were obtained from the mentioned aqueous solutions and two different TTCP/DCPA molar ratios.

The IS technique was used as a tool to describe the main microstructural characteristics developed from the prepared formulations. An equivalent circuit that takes into account the main features of the expected structures was proposed to fit the impedance experimental data, relating the circuit elements to the microstructural characteristics. This approach was shown to be very useful to relate the cement compositions to the obtained microstructures.

2 Materials and methods

2.1 Preparation of the calcium phosphate cements

Commercially available DCPA from Sigma–Aldrich (99% purity) was used as received. The synthesis of TTCP from reagent-grade $CaCO_3$ (Mallinckrodt, P.A. A.C.S., 99% purity) and $(NH_4)_2HPO_4$ (Merck, P.A. A.C.S., 99% purity) was described elsewhere [19].

DCPA and TTCP specific surface areas were 1.52 and 0.32 m^2/g, respectively. Two CPC powders with different TTCP/DCPA molar ratios (1/1 and 1/2) were prepared as the solid phases of the cements. Three different aqueous solutions (5% volume fraction) of $Na_2HPO_4 \cdot 12\ H_2O$ (Cicarelli, P.A. A.C.S., 99% purity), (L+) tartaric acid (Cicarelli, P.A. A.C.S., 99% purity) and oxalic acid dihydrate (Cicarelli, P.A. A.C.S., 99.5% purity) were used as the liquid phases for each TTCP/DCPA molar ratio. The samples (see Table 1) were prepared by mixing 1.3 g of

Table 1 Composition of the cements

Sample	TTCP:DCPA molar ratio	Liquid phase (5% volume fraction)	Powder/liquid ratio (g/ml)
P 1:1	1:1	Na_2HPO_4	3
P 1:2	1:2		
T 1:1	1:1	Tartaric acid	2.6
T 1:2	1:2		
O 1:1	1:1	Oxalic acid	2.3
O 1:2	1:2		

cement powder with the required amount of liquid phase to obtain workable pastes, which were placed in a polystyrene mould (1.14 cm × 0.50 cm in diameter and height) and stored in a 100% relative humidity incubator at 37 ± 1°C for 24 h. Finally, the hardened samples were removed from the moulds and polished by a fine abrasive paper to be analyzed. The final dimensions of the polished cement bodies were 1.138 cm × 0.30 cm in diameter and height.

2.2 Analysis and characterization methods

The BET method was used to determine the specific surface area (SSA) of the calcium phosphates. SSA was measured by nitrogen adsorption on the particle surfaces with a Micromeritics Flowsorb II 2300 device.

Crystalline phases of the cements were determined by X-ray powder diffraction (XRD, Philips 1830/00) with Ni-filtered Cu Kα radiation ($\lambda = 1.54050$ Å). The electrical voltage and current were 40 kV and 30 mA, respectively. Data were collected for 2θ ranging between 10° and 70° with a step size of 1°/min.

Fourier transformed infrared (FTIR) spectra were recorded with a Genesis II-Mattson device in the transmittance mode, in the range 400–4000 cm^{-1} with a resolution of 2 cm^{-1}. Spectra were obtained using pellets of the crushed cements with KBr.

Scanning electron microscopy (SEM, Jeol JXA-8600) was used to analyze the developed microstructures in the cement samples after coating them with a fine gold layer.

Apparent densities of the cements were determined from the volume of the specimens and their masses obtained with a Sartorius YDK 01 balance. Three samples of each composition were used.

Initial and final setting times of the cement pastes were determined with Gillmore needles according to the ASTM standard C266-99. The setting times, obtained from a set of three samples of each cement, are expressed as mean ± standard error of the mean. Statistical analysis was performed on the experimental data by means of a Student's *t*-test.

Impedance spectroscopy (IS) measurements were carried out by means of an HP 4284A LRC meter with an amplitude voltage of 0.5 V in the frequency range from 20 Hz to 1 MHz at room temperature. Silver electrodes were deposited on both faces of the hardened samples in order to study the electrical response of the different cement systems.

3 Results and discussion

3.1 Setting times of the cements

The success and applicability of calcium phosphate cements in dental and medical restorations are dependent on many physicochemical and biological aspects. In this way, the setting of these systems is strongly related to the clinical demands. A long period of plasticity is, sometimes, beneficial to the handling of the paste, the CPC being prepared at the required moment and applied when needed. However, relatively short setting times are frequently needed in common surgical procedures.

Initial and final setting times of the samples are plotted as column graphs in Fig. 1. The statistical analysis showed no differences between the initial times (~12 min) corresponding to the samples prepared using Na_2HPO_4 (P 1:1 and P 1:2) and oxalic acid (O 1:1 and O 1:2) solutions as the liquid phases, whereas the samples prepared from tartaric acid solution (T 1:1 and T 1:2) showed the longest initial setting times. Regarding the final setting times, the samples O 1:1 and O 1:2 showed the shortest values (~20 min) comparing to the other cements.

The fact that the formulations prepared from oxalic acid showed the shortest initial and final setting times was attributed to the pH-lowering effect associated to the

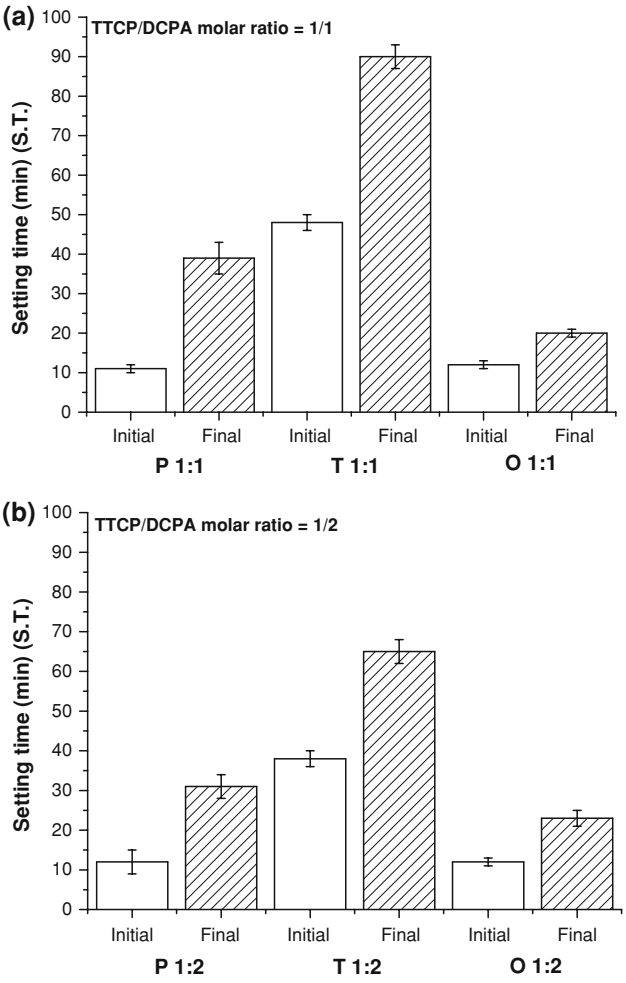

Fig. 1 Initial and final setting times of the developed cements

presence of this acid. The acidic conditions facilitate the dissolution of the reactants. After that, the precipitation and entanglement of the formed crystals lead to the setting and final hardening of the cements. Moreover, we think that the low value corresponding to the initial setting time (in both cements) could be associated to the formation of insoluble calcium oxalate salts during the first stages of the setting process, whereas the final setting would be mainly related to the precipitation of hydroxyapatite, which occurs at higher pH values. As a result, these two effects could act consecutively thus imparting a fast setting and hardening to the cement pastes. On the base of the measured setting times, we observed that the values obtained from the oxalic acid-based cements are very similar to those corresponding for one of the commercially available cements (*Biocement-H*). This cement is made up of 98 wt% α-TCP (minor contents of β-TCP) and 2 wt% precipitated hydroxyapatite as crystal seeds. Its liquid phase is an aqueous solution of 2.5 wt% disodium hydrogen phosphate. The setting times reported in the literature for this bone cement are about 8 min and 20 min for the initial and final times, respectively [20]. This demonstrates that the oxalic acid solution provides a strong accelerator effect without needing the incorporation of crystal seeds into the formulation. The final setting of the oxalic acid-based cement was accelerated in a factor between 2 (when compared with P 1:1 sample) and 5.5 (when compared with T 1:1 sample), when an equimolar mixture of calcium phosphates was employed in the solid phase.

Regarding the effect of changing the TTCP/DCPA molar ratio on the setting times, it must be pointed out that final times decrease when changing the cement composition from 1/1 to 1/2, both when using Na_2HPO_4 and tartaric acid solutions. No changes were observed (within the experimental error) when the oxalic acid solution was employed as the liquid phase.

3.2 X-ray powder diffraction (XRD) analysis

Figure 2 shows the X-ray patterns corresponding to set P 1:1, T 1:1 and O 1:1 cements, after 24 h in a 100% relative humidity incubator at 37 ± 1°C.

The diffractograms corresponding to P 1:1 and O 1:1 specimens show the formation of low-crystallinity hydroxyapatite as the main phase as well as unreacted DCPA and TTCP. It should be noted that acidic DCPA is the reactant preferentially consumed when the more basic Na_2HPO_4 solution is employed as the setting liquid (P 1:1 sample), leaving TTCP practically unreacted. On the other hand, it is clearly observed how TTCP (the basic reactant in the solid mixture) patterns decrease their intensity as a consequence of using the more acidic solution in O 1:1 cement. The peaks corresponding to crystalline calcium

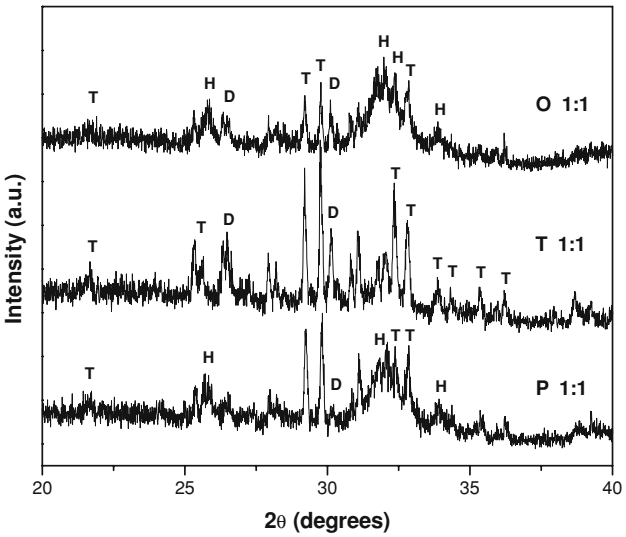

Fig. 2 XRD diffractograms corresponding to the cements prepared from an equimolar mixture of the calcium phosphates. References: H (Hydroxyapatite), T (TTCP) and D (DCPA)

oxalate phase were not detected in this sample. After 24 h, the T 1:1 cement showed no noticeable conversion to hydroxyapatite. Only DCPA and TTCP patterns could be identified in the diffractogram, whereas the patterns corresponding to calcium tartrate phase were not detected. Similar qualitatively results were obtained for the cements prepared from a TTCP/DCPA = 1/2 molar ratio.

In summary, from XRD analyses we observed that it is possible to control the specific consumption of one of the calcium phosphate reactants in the solid mixture depending on the pH of the solution used as the liquid phase. As a consequence, it is possible to control the workable time of the paste as well as the setting times of the cements. This could be very useful when preparing the relative amounts of each solid component in the mixture and when selecting the liquid phase to be used according to the clinical requirements.

3.3 Fourier transformed infrared (FTIR) spectroscopy analysis

Figure 3 depicts the FTIR spectra of the cements prepared by using a TTCP/DCPA equimolar ratio. The small shoulder located at about 3570 cm^{-1} (overlapped with a wide band centred at 3340 cm^{-1} corresponding to the presence of water) was assigned to the OH stretching in the structure of hydroxyapatite [21], corresponding to the samples P 1:1 and O 1:1. In sample T 1:1 this peak was not detected.

In all samples, a wide band centred at about 1060 cm^{-1} was attributed to the asymmetric P–O stretching in the structure corresponding to PO_4^{3-} groups (both those of the hydroxyapatite structure and those of the reactants) [21].

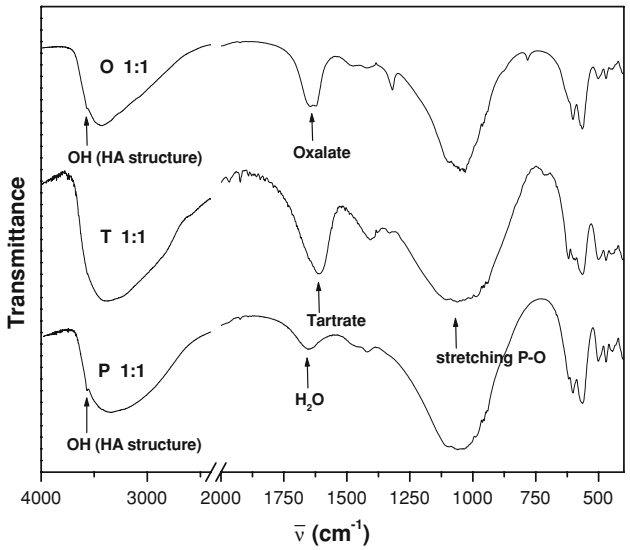

Fig. 3 FTIR spectra corresponding to the cements prepared from an equimolar mixture of the calcium phosphate reactants

The low-intensity band located at 1640 cm^{-1} was assigned to the presence of water in sample P 1:1, whereas the shifted band at about 1600 cm^{-1} in sample T 1:1 was attributed to the asymmetric stretching vibration of the two equivalent carbon–oxygen bonds corresponding to the calcium tartrate structure [22]. On the other hand, in the sample prepared from oxalic acid solution, the band located at 1630 cm^{-1} was assigned to the calcium oxalate structure. These facts support the hypothesis that these organic salts would contribute to the setting process in these cements. However, taking into account the values corresponding to the initial and final setting times of the samples prepared from tartaric acid, it is possible to infer that the formed calcium tartrate could be deposited on the reactant surfaces, hindering the dissolution of the calcium phosphates. This could explain both the low conversions to hydroxyapatite and the long setting times measured in these cements (T 1:1 and T 1:2). On the other hand, the formation of calcium oxalate does not seem to inhibit the formation of low-crystallinity hydroxyapatite (as can be seen from XRD analyses). Similar results were obtained from the FTIR spectra corresponding to the cements prepared from a TTCP/DCPA = 1/2 molar ratio.

3.4 Scanning electron microscopy (SEM) observations and apparent densities

SEM images of the cement fracture surfaces and apparent densities of the samples are shown in Fig. 4. It is possible to observe the different developed microstructures as well as the presence of some unreacted phases. Thus, the density values were related to the presence of these unreacted phases as well as to both the different degree of conversion to hydroxyapatite and developed porosity. What is very interesting to note is the different degree of entanglement and crystal size developed in each specimen depending upon the accelerator used.

The structures obtained from tartaric acid are made up of different phases like unreacted DCPA and TTCP, whereas small amounts of little crystals (which could be attributed to calcium tartrate) were also observed. Non-homogeneous microstructures with a low-degree of entanglement were developed in both cases (T 1:1 and T 1:2). This could explain the long setting times and low conversions to hydroxyapatite obtained for these systems. This led to a low mechanical resistance which was detected when samples were removed from the moulds.

When Na_2HPO_4 was used in the liquid phase, very small crystals were observed in the cement P 1:1, due probably to the precipitation of hydroxyapatite on the surface of the TTCP particles (taking into account that this phase remained practically unreacted, according to the XRD analysis). This cement showed both the largest pore size and the most homogeneous microstructure in comparison with the other samples. Cement P 1:2 showed a closer microstructure than that of P 1:1 as well as an unreacted phase which was attributed to DCPA (up and left on the image).

The cement prepared from an equimolar mixture of TTCP and DCPA and oxalic acid as accelerator presented a homogeneous structure with both large hydroxyapatite crystals and high degree of entanglement, showing a smaller mean pore size than that of P 1:1 sample. On the other hand, inhomogeneities were observed in sample O 1:2 which were again attributed to the presence of unreacted DCPA particles, in agreement to the corresponding XRD diffractogram.

Regarding the porosity of the prepared samples, it is known that the powder-to-liquid ratio affects strongly this microstructural feature in CPCs. In fact, increasing the powder-to-liquid ratio will result in a more porous material, which entirely agrees with the presented results (see Table 1 and Fig. 4).

The calcium phosphate cements developed in this work have fewer components than those employed in bone cements frequently reported in the literature. The proposed formulations contain neither hydroxyapatite crystal seeds [23], nor fibers [24], nor gelling agents [12] as constituents. Despite this, high conversions to low-crystallinity hydroxyapatite and short setting times were obtained for those cements developed from Na_2HPO_4 and oxalic acid solutions.

3.5 Microstructural analysis by impedance spectroscopy (IS)

In recent years, the IS technique has been shown to be a very sensitive tool to reveal changes in the developed

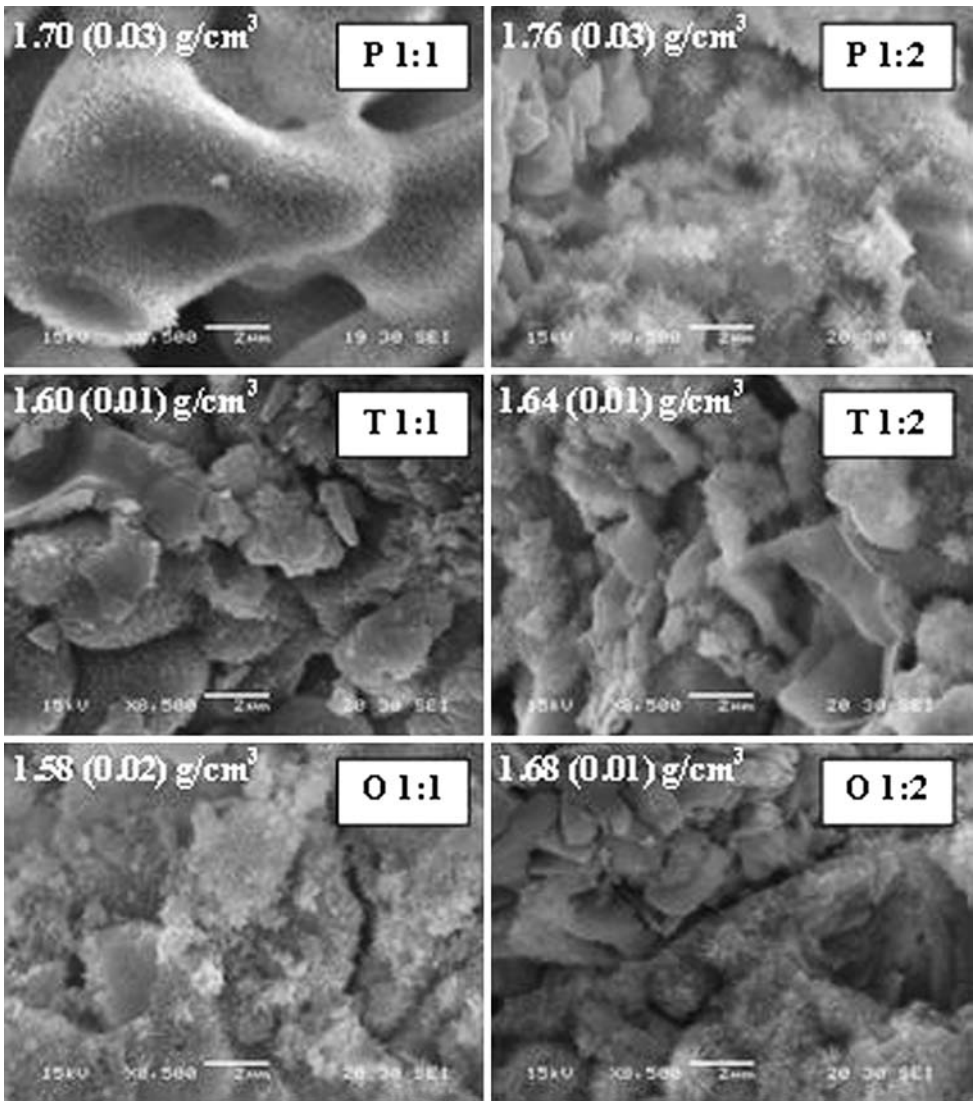

Fig. 4 SEM micrographs of the cement fracture surfaces and apparent densities (standard deviations are indicated into parentheses)

microstructures of Portland cement [14–16]. On the other hand, only few reports have been focused on employing this technique to analyse deeply the microstructural changes of bone cements, aiming to the improvement of these systems in the biomaterials area [25, 26]. One of the most important advantages of IS technique is its non-destructive character. For all these reasons, IS was used in the present work to obtain valuable information related to porosity, tortuosity and homogeneity of the cement microstructures.

It is possible, for simplicity, during the impedance analysis of the systems studied here, to divide the complex diagrams, i.e. Nyquist curves, into two regions [15, 26]: the low-frequency region which is frequently related to the polarization occurring at the cement/electrode interfaces, and the high-frequency region assigned to the bulk response. The low-frequency region is composed by only one relaxation process, while the high-frequency one is composed by two distinct relaxations. This work was focused on the high-frequency region from where the microstructural features of the cements can be studied in details, i.e. information concerning the bulk of the cements can be obtained. Generally, in terms of an equivalent circuit representation, a parallel resistance and capacitance can be used to deal with the electrode/cement contact. However, as previously commented, the study of the electrode/cement interface is not the subject of the present work. On the other hand, bulk properties were carefully analyzed and the information given from this part of the impedance spectra was used as a tool to understand the microstructural characteristics developed in the cements, as a consequence of the setting and hardening processes.

Figure 5a depicts the equivalent circuit employed to fit the experimental data obtained from the impedance spectra. In this figure, the R_b and C_b are the ionic resistance and capacitance of the bulk of the cements [25, 26], respectively. The R_b is indeed related to the ionic transport along the connected and percolated pores. The series $r_{t,i}$ and $c_{t,I}$ represent the blocking ionic path along of the system or

material [27]. In other words, they represent different closed (occluded) pores of different sizes which act as a blocking phase to the ionic transport along of the material. This phase (closed and occluded pore phase) is likely distributed and can be also treated as a Constant Phase Element (CPE), i.e. a continuous distribution of series $r_{t,i}$ and $c_{t,I}$ can be treated as a CPE element. Indeed, note that this equivalent circuit is an universal circuit well described by Jonscher [28]. Therefore, here, the series $r_{t,i}$ and $c_{t,I}$ represent the "dielectric relaxation process" associated to the blocking ionic conductivity of occluded pores.

The Nyquist impedance diagrams for the above mentioned systems are shown here in Fig. 5b–d, i.e. they correspond to the cements prepared by using Na_2HPO_4, tartaric acid and oxalic acid as liquid phases, respectively. From the fitting of the experimental data to the model it is possible to separate the electrode response from that of bulk, i.e. it is possible to distinguish the bulk and to analyze it separately. Indeed, the C_b accounts for the dielectric capacitance associated to the solid phase (cement matrix, see Fig. 6). Table 2 lists some of the parameters obtained from the fitting of the impedance experimental data corresponding to the developed cements.

Regarding the systems made from the Na_2HPO_4 solution (P 1:1 and P 1:2), the rise in apparent density as the composition of the formulation goes from TTCP/DCPA = 1/1 to 1/2, is clearly seen (Fig. 4). This lower porosity corresponding to P 1:2 can also be detected from the apparent dielectric constant (see Table 2), obtained as follows:

$$\varepsilon = C_b \cdot d/\varepsilon_0$$

where d is the sample thickness (0.3 cm) and ε_0 is the vacuum permittivity (8.85×10^{-14} F cm^{-1}). The dependence of C_b (and thus, ε) on the porosity of the sample has been already reported elsewhere [29]. Then, the apparent dielectric constant increases as the porosity of the cement decreases. As a result, it is possible to say that employing 2 mol of DCPA per mol of TTCP, a less-porous cement matrix is obtained when using a Na_2HPO_4 solution as the accelerator agent ($\varepsilon = 9.37$ for P 1:2 and $\varepsilon = 7.67$ for P 1:1).

As to the tortuosity of the crossing pores in the cements, it can be related to the values corresponding to the bulk cement resistance. As the hydration proceeds, the pore structure becomes higher tortuous leading to a higher bulk

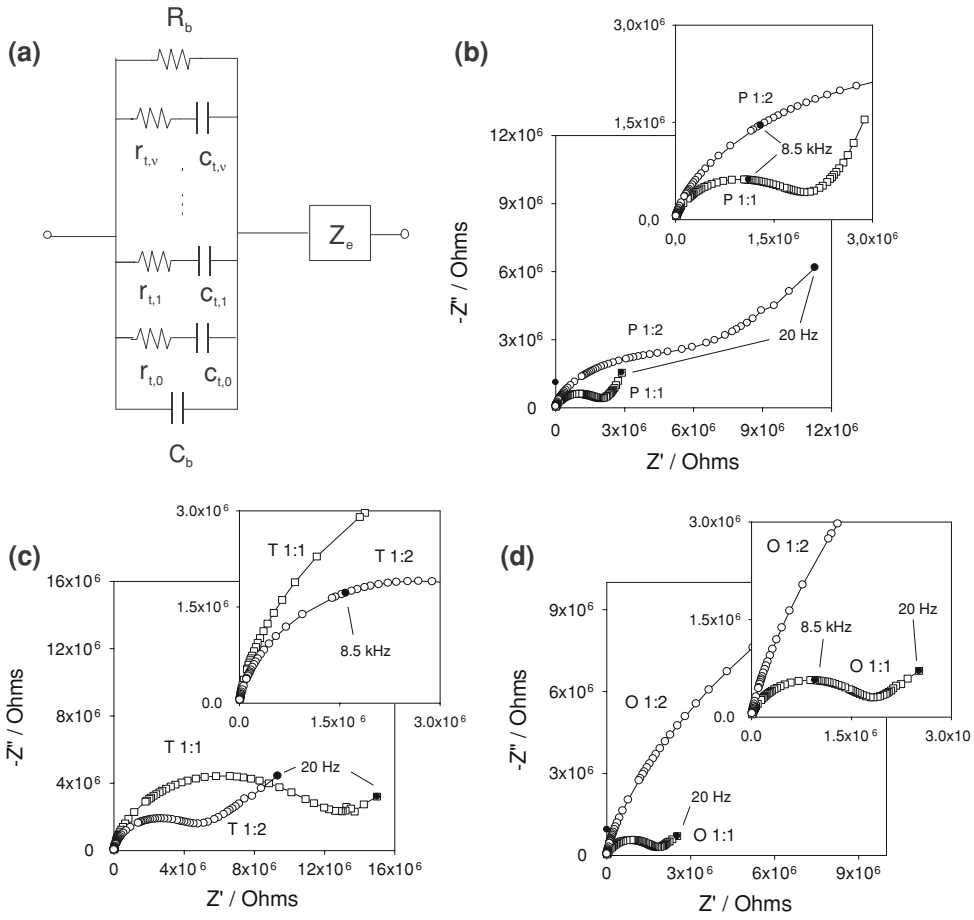

Fig. 5 **a** Equivalent circuit employed to fit the impedance experimental data. The Z_e is the impedance related to the electrode polarization at electrode/electrolyte interface. The physical interpretation of the other elements is discussed along the text. Nyquist impedance diagrams corresponding to: **b** Na_2HPO_4-based cements, **c** tartaric acid-based cements, and **d** oxalic acid-based cements. In this figure, the insets show in details the high frequency region

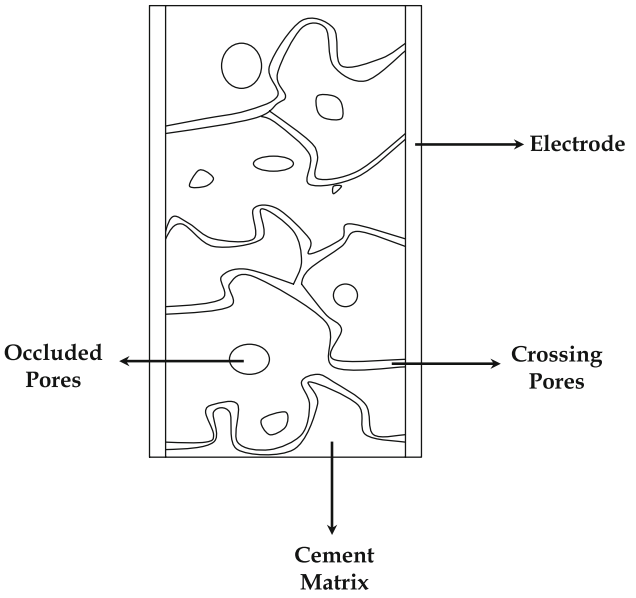

Fig. 6 Microstructural features of the cements according to the physical interpretation arose from impedance spectroscopy analysis

Table 2 Parameters obtained from the fitting of the impedance experimental curves

Sample	Apparent dielectric constant	Bulk cement resistance (ohms)	Arc depression factor
P 1:1	7.67	2.61×10^6	0.52
P 1:2	9.37	7.50×10^6	0.52
T 1:1	7.73	1.30×10^7	0.60
T 1:2	11.11	5.23×10^6	0.57
O 1:1	8.89	1.86×10^6	0.58
O 1:2	9.26	3.95×10^7	0.61

resistance. From the analysis of these values we inferred that the microstructure developed in P 1:2 sample must be higher tortuous than that corresponding to P 1:1 sample. It is important to mention that it has been considered, as an approximation, the same conductivity of the liquid phase filling the pores after 24 h setting for both formulations. The different values obtained for the bulk resistance can also be related to the amount of liquid-connected phase, e.g. to the porous characteristics of the system, i.e. distribution, length and diameter. A lower porosity density shall lead to a higher resistance [26], which is consistent with the results obtained by SEM analysis for the studied samples. Then these facts, both the tortuosity and porosity density, are capable to qualitatively justify the differences found in the bulk resistance values. Therefore, by using a TTCP/DCPA = 1/1 molar ratio, a more-porous and open microstructure with less-tortuous (more connected) crossing pores is obtained in comparison to the 1/2 molar ratio, when a Na_2HPO_4 solution is employed as the liquid phase of the cement paste. These facts could be attributed to the agglomerates of DCPA observed by SEM, which would act as barriers blocking and increasing the effective pore paths.

Regarding the arc depression factor, it has been suggested that this parameter is a measure of the microstructural inhomogeneity of the cement pastes (thus related to the pore size distribution) [15]. In this way, the closer the value of this parameter to unity the more homogeneous the microstructure, or in other words, the narrower the pore size distribution (in length and/or diameter). Based on this analysis, it is possible to observe that there are no differences between the values corresponding to P 1:1 and P 1:2. This means that both cements exhibit a wide pore size distribution in the cement matrix.

Accordingly, from the results corresponding to the samples made from the oxalic acid solution, we inferred that the O 1:1 formulation developed a more-porous and less-tortuous microstructure in comparison with O 1:2. On the other hand, in this case, both cements exhibit a narrower pore size distribution than that corresponding to the samples prepared from Na_2HPO_4. This fact is supported by the higher values of the arc depression factors, although these cements showed a small pore size as evaluated from SEM images.

Finally, concerning the impedance diagrams corresponding to the cements prepared from tartaric acid, it is clearly seen that although T 1:1 sample is more porous than T 1:2, the bulk resistance value obtained for the equimolar composition is higher than that of T 1:2. This could be explained considering more-tortuous crossing pore paths for T 1:1 cement, although no differences could be observed from SEM images since both cements developed inhomogeneous microstructures.

A detailed analysis of the microstructure and biological behaviour of the CPCs developed in this study incorporating drug-containing hybrid microspheres as drug carriers is currently in progress.

4 Conclusions

The IS technique has been used as a non-destructive tool to evaluate the effect of different setting accelerator agents on the developed microstructures of CPCs which could be employed in medical restorations. Six compositions of CPCs were prepared from two different TTCP/DCPA molar ratios (as the solid phases) and three different aqueous solutions (as the liquid phases). The formulations prepared from a TTCP/DCPA equimolar mixture and oxalic acid-based liquid phase presented the shortest initial and final setting times (12 and 20 min, respectively) in comparison with the other studied systems (Na_2HPO_4-based and tartaric acid-based cements). Both high

conversions to low-crystallinity hydroxyapatite and the presence of calcium oxalate salts were determined from XRD and FTIR analyses in the cements prepared from oxalic acid as the liquid phase. High degree of entanglement of the formed crystals was observed by SEM in samples containing oxalic acid. In all developed cements, changes in porosity, tortuosity and microstructural homogeneity were determined, by employing the IS technique, when the TTCP/DCPA molar ratio was changed from 1/1 to 1/2. An equivalent circuit that takes into account the main features of the cement microstructures was proposed to fit the impedance experimental data. This approach was very useful to relate the cement composition to the obtained microstructure and it could be employed as a valuable tool when designing a new cement formulation to be used according to the specific clinical requirements.

Acknowledgements Authors would like to thank the financial support of the following institutions: National Research Council (CONICET, Argentina), National Agency for the Promotion of Science and Technology (ANPCyT, Argentina, PICT 12-14593), University of Mar del Plata and Fundación Antorchas (Argentina).

References

1. Brown BW, Chow LC. Dental restorative cement paste. US Patent No. 4.518.430; 1985.
2. Brown PW, Fulmer M. Kinetics of hydroxyapatite formation at low temperature. J Am Ceram Soc. 1991;74:934–40.
3. Matsuda S, Takagi S, Chow LC. Effects of mixing ratio and pH on the reaction between $Ca_4(PO_4)_2O$ and $CaHPO_4$. J Mater Sci: Mater Med. 2000;11:305–11.
4. Barralet JE, Grover L, Gaunt T, Wright AJ, Gibson IR. Preparation of macroporous calcium phosphate cement tissue engineering scaffold. Biomaterials. 2002;23:3063–72.
5. Miao X, Hu Y, Liu J, Wong AP. Porous calcium phosphate ceramics prepared by coating polyurethane foams with calcium phosphate cements. Mater Lett. 2004;58:397–402.
6. Xu HHK, Carey LE, Simon CG Jr, Takagi S, Chow LC. Premixed calcium phosphate cements: synthesis, physical properties and cell cytotoxicity. Dent Mater. 2007;23:433–41.
7. Yu D, Wong J, Matsuda Y, Fox JL, Higuchi W, Otsuka M. Self-setting hydroxyapatite cement: a novel skeletal drug-delivery system for antibiotics. J Pharmac Sci. 1992;81:529–32.
8. Fukase Y, Eanes ED, Takagi S, Chow LC, Brown WE. Setting reactions and compressive strengths of calcium phosphate cements. J Dent Res. 1990;69:1852–6.
9. Bohner M, Gbureck U, Barralet JE. Technological issues for the development of more efficient calcium phosphate bone cements: a critical assessment. Biomaterials. 2005;26:6423–9.
10. Yoshikawa M, Toda T. In vivo estimation of periapical bone reconstruction by chondroitin sulphate in calcium phosphate cement. J Eur Ceram Soc. 2004;24:521–31.
11. Xu HHK, Simon CG Jr. Fast setting calcium phosphate-chitosan scaffold: mechanical properties and biocompatibility. Biomaterials. 2005;26:1337–48.
12. Carey LE, Xu HHK, Simon CG Jr, Takagi S, Chow LC. Premixed rapid-setting calcium phosphate composites for bone repair. Biomaterials. 2005;26:5002–14.
13. Ginebra MP, Traykova T, Planell JA. Calcium phosphate cements as bone drug delivery systems: a review. J Control Release. 2006;113:102–10.
14. Xu Z, Gu P, Xie P, Beaudoin JJ. Application of AC impedance techniques in studies of porous cementitious materials: III. ACIS behavior of very low porosity cementitious systems. Cem Concr Res. 1993;23:1007–15.
15. Christensen BJ, Coverdale RT, Olson RA, Ford SJ, Garboczi EJ, Jennings HM, et al. Impedance spectroscopy of hydrating cement-based materials: measurement, interpretation, and application. J Am Ceram Soc. 1994;77:2789–804.
16. Coverdale RT, Christensen BJ, Jennings HM, Mason TO, Bentz DP, Gaboczi EJ. Interpretation of impedance spectroscopy of cement paste via computer modelling. J Mater Sci. 1995;30:712–9.
17. Liu CS, Hu LM. A.C. Impedance technique-A new method to determine the changes of microstructure in the process of cement hydration in situ. Chin Chem Eng Prog. 1997;5:23–6.
18. Prentice LH, Tyas M. The effect of oxalic acid incorporation on the setting time and strength of a glass-ionomer cement. Acta Biomater. 2006;2:109–12.
19. Romeo HE, Fanovich MA. Synthesis of tetracalcium phosphate from mechanochemically activated reactants and assessment as a component of bone cements. J Mater Sci: Mater Med. 2008;19:2751–60.
20. Fernández E, Vlad MD, Monserrat Gel M, López J, Torres R, Cauich JV, et al. Modulation of porosity in apatitic cements by the use of α-tricalcium phosphate-calcium sulphate dihydrate mixtures. Biomaterials. 2005;26:3395–404.
21. Brown PW, Constantz B. Hydroxyapatite and related materials. Boca Raton, USA: CRC Press; 1994.
22. Colthup NB, Daly LH, Wiberley SE. Introduction to infrared and raman spectroscopy. New York: Academic Press; 1975.
23. Liu CS, Shen W. Effect of crystal seeding on the hydration of calcium phosphate cement. J Mater Sci: Mater Med. 1997;8:803–7.
24. Xu HHK, Quinn JB. Calcium phosphate cement containing resorbable fibers for short-term reinforcement and macroporosity. Biomaterials. 2002;23:193–202.
25. Liu C, Huang Y, Zheng H. Study of the hydration process of calcium phosphate cement by AC impedance spectroscopy. J Am Ceram Soc. 1999;82:1052–7.
26. Kim S, Hwang JH. Application of impedance spectroscopy to cement-based materials: hydration of calcium phosphate bone cements. J Kor Ceram Soc. 2006;43:156–61.
27. Raistrick ID, Mcdonald JR, Franceschetti DR. In: Macdonald JR, editor. Impedance spectroscopy: emphasizing solid materials and systems (chapter 2). New York: Wiley; 1987.
28. Jonscher AK. The 'universal' dielectric response. Nature. 1977;267:673–9.
29. Andrade C, Blanco VM, Collazo A, Keddam M, Novoa XR, Takenouti H. Cement paste hardening process studied by impedance spectroscopy. Electrochem Acta. 1999;44:4313–8.